Available online at www.sciencedirect.com
SCIENCE DIRECT
Coastal Engineering 53 (2006) 573–588
Coastal Engineering
An International Journal for Coastal, Harbour and Offshore Engineers
www.elsevier.com/locate/coastaleng

Empirical parameterization of setup, swash, and runup

Hilary F. Stockdon [a,*], Rob A. Holman [b], Peter A. Howd [a], Asbury H. Sallenger Jr. [a]

[a] Center for Coastal and Watershed Studies, U. S. Geological Survey, St. Petersburg, FL, United States
[b] College of Oceanic and Atmospheric Sciences, Oregon State University, Corvallis, OR, United States

Received 27 May 2005; received in revised form 19 December 2005; accepted 21 December 2005
Available online 21 February 2006

Abstract

Using shoreline water-level time series collected during 10 dynamically diverse field experiments, an empirical parameterization for extreme runup, defined by the 2% exceedence value, has been developed for use on natural beaches over a wide range of conditions. Runup, the height of discrete water-level maxima, depends on two dynamically different processes; time-averaged wave setup and total swash excursion, each of which is parameterized separately. Setup at the shoreline was best parameterized using a dimensional form of the more common Iribarren-based setup expression that includes foreshore beach slope, offshore wave height, and deep-water wavelength. Significant swash can be decomposed into the incident and infragravity frequency bands. Incident swash is also best parameterized using a dimensional form of the Iribarren-based expression. Infragravity swash is best modeled dimensionally using offshore wave height and wavelength and shows no statistically significant linear dependence on either foreshore or surf-zone slope. On infragravity-dominated dissipative beaches, the magnitudes of both setup and swash, modeling both incident and infragravity frequency components together, are dependent only on offshore wave height and wavelength. Statistics of predicted runup averaged over all sites indicate a −17 cm bias and an rms error of 38 cm: the mean observed runup elevation for all experiments was 144 cm. On intermediate and reflective beaches with complex foreshore topography, the use of an alongshore-averaged beach slope in practical applications of the runup parameterization may result in a relative runup error equal to 51% of the fractional variability between the measured and the averaged slope.
Published by Elsevier B.V.

Keywords: Wave runup; Swash; Wave setup; Remote sensing

1. Introduction

When ocean waves approach a coast, the majority of wave energy is dissipated across the surf zone by wave breaking. However, a portion of that energy is converted to potential energy in the form of runup on the foreshore of the beach (Hunt, 1959). This wave runup is important to coastal planners, nearshore oceanographers, and coastal engineers because these motions deliver much of the energy responsible for dune and beach erosion (Ruggiero et al., 2001; Sallenger, 2000). Thus, understanding the magnitude and longshore variability of extreme runup is critical to accurate prediction of the impacts on protective dunes and adjacent properties. The goal of this work is to devise a simple parameterization for maximum runup elevation, improving upon an earlier empirical formula for wave runup by Holman (1986). These elevations, in turn, can be used as input into a storm impact model (Sallenger, 2000).

In the discussion below, it will be apparent that wave height, H, deep-water wave length, L_0, wave period, T, and beach steepness, β, form a commonly accepted environmental parameter set. Of these, deep-water wavelength and period are assumed to be interdependent, linked by the linear dispersion relationship,

$$L_0 = \frac{gT^2}{2\pi}. \quad (1)$$

The three independent parameters may provide a first-order description of a beach environment and are often expressed in

* Corresponding author. Tel.: +1 727 803 8747x3074; fax: +1 727 803 2032.
E-mail address: hstockdon@usgs.gov (H.F. Stockdon).

0378-3839/$ - see front matter. Published by Elsevier B.V.
doi:10.1016/j.coastaleng.2005.12.005

terms of a non-dimensional surf similarity parameter, commonly called the Iribarren Number (Battjes, 1974),

$$\xi = \frac{\beta}{(H/L_0)^{1/2}}. \quad (2)$$

The Iribarren number can be interpreted as a dynamic beach steepness, comparing beach slope to the square root of deep-water wave steepness.

In early laboratory experiments of monochromatic waves on planar beaches, all quantities were well defined. However, application of this scaling to natural beaches introduces several complications. For random waves, both wave period and wave height become statistical measures, often described by the peak period, T_p, and the root mean square (rms) or significant wave height, H_{rms} or H_s, (defined as 2.8 and 4 times the standard deviation of the time series of sea-surface elevation, respectively). Additionally, wave-height measures can be expressed in deep water (H_0), at the break point (H_b), or locally. Definition of a single beach slope becomes difficult on natural beaches with typically concave profiles and is further complicated by the common presence of offshore sandbars. Estimation of runup statistics under these complicated conditions may be handled by appropriate numerical models along with knowledge of boundary conditions (Raubenheimer and Guza, 1996; Raubenheimer et al., 1995) such as the full incident wave spectra and bottom bathymetry. However, such an approach is incompatible with broad application to coastal zone management problems because details of the offshore profile and incident spectra are not always available. Therefore, we will investigate the degree to which simple parameterizations provide useful predictions of extreme runup on natural beaches.

2. Background

Runup, $R(y,t_i)$, is defined here as the set of discrete water-level elevation maxima (Fig. 1a), measured on the foreshore, with respect to still water level (that which would occur in the absence of waves). The values of runup depend on the longshore location, y, time, t, and the discrete times of maxima, t_i. Runup results from two dynamically different processes: (1) maximum setup, $\langle\eta\rangle(y)$, the time-averaged water-level elevation at the shoreline, and (2) swash, $S(y,t_i)$, the time-varying, vertical fluctuations about the temporal mean (Fig. 1a).

Setup, the super-elevation of the mean water level, is driven by the cross-shore gradient in radiation stress that results from wave breaking (Longuet-Higgins and Stewart, 1963, 1964). The relationships between setup and environmental conditions, and resulting expressions for setup at the shoreline, have been the topics of many research studies. Bowen et al. (1968) wrote a simplified expression for setup by assuming normally incident shallow-water waves whose height within the surf zone was limited to a constant fraction of the local water depth, $\gamma = H/h$. The resulting expression was

$$\frac{\langle\eta\rangle}{H_b} = 0.38\gamma, \quad (3)$$

where H_b is the breaking wave height. Measured setup values were found to be greater than that predicted by theory due to the

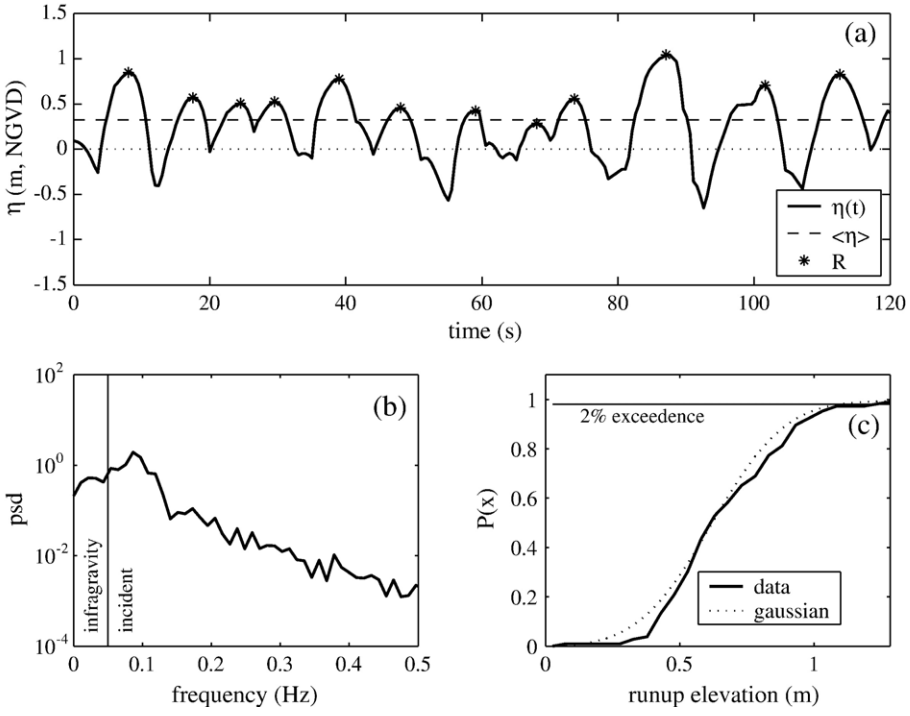

Fig. 1. Water-level time series (a), extracted from timestack in Fig. 2, indicating individual runup maxima, R, setup at the shoreline, $\langle\eta\rangle$, and swash excursion, S. Significant swash statistics, S, were calculated from the spectra (b) of the water-level time series. The 2% exceedence value of runup, R_2, was calculated from the cumulative PDF of the discrete measures of R (c).

asymptotic approach of setup to the beach surface (Bowen et al., 1968). Examining data from gently sloping beaches of southern California, Guza and Thornton (1981) found $<\eta>$ to be proportional to the significant wave height (10-m depth), H_s, with a constant of proportionality equal to 0.17. In contrast, analysis of data from a beach in Duck, NC (Holman and Sallenger, 1985) showed that a direct correlation between setup and wave height was highly scattered and that non-dimensional setup (normalized by offshore wave height) scaled better with the Iribarren number, ξ_0. The Guza and Thornton (1981) data were found to be consistent with the Holman and Sallenger (1985) relationship at low Iribarren numbers. While the Holman and Sallenger (1985) relationship between ξ_0 and $<\eta>$ significantly reduced the scatter in the data, there remained a tidal dependence. The relationship failed during the lowest tides when waves significantly dissipated over an offshore sandbar. Using observations of setup on beaches in Australia, Hanslow and Nielsen (1993) found that the maximum setup on dissipative beaches showed no dependence on beach slope and, therefore, could not be scaled with ξ_0.

Swash, S, is generally defined as the time-varying location of the intersection between the ocean and the beach. According to Miche (1951), monochromatic waves are composed of two parts: a progressive component whose energy is dissipated during wave breaking and a standing, reflected component that has its maximum at the shoreline. Swash represents this standing component whose amplitude cannot exceed some critical value that is dependent on both β and T_0. Early studies on swash and runup were conducted in laboratories in order to determine the impacts of waves on structures. Based on Miche's ideas, Hunt (1959) stated that there is a critical wave steepness below which wave energy will be totally reflected by a beach with a planar slope. Under surging wave conditions, there is little dissipation of wave energy across the beach slope, and the majority of the energy is reflected on the steep beach slope (Hunt, 1959). For the more common situation of breaking waves, energy is dissipated across the surf zone. Using a critical value based on wave steepness and β (Iribarren and Nogales, 1949), which defines a threshold between breaking and non-breaking conditions, Hunt (1959) proposed an empirical formulation for vertical wave up-rush, R, that can be re-written in terms of ξ,

$$\frac{R}{H} = K\xi, \tag{4}$$

where Hunt assumes that $H \approx H_0$.

Using field data collected from Duck, NC, Holman (1986) found a clear relationship between 2% exceedence value of runup, R_2, normalized by H_s (in 18-m depth) and ξ_0,

$$\frac{R_2}{H_s} = 0.83\xi_0 + 0.2, \tag{5}$$

which includes a linear dependence on the foreshore beach slope, β_f. For experiments on natural beaches, wave breaking over offshore sandbars can significantly attenuate offshore waves. Thus, coefficients from data gathered at a single experiment (such as in Eq. (5)) may vary with sandbar configuration and profile shape, introducing significant amounts of noise into empirical relationships. Baldock and Holmes (1999) found in numerical simulations that incident band swash saturation was related to bore-driven swash, which also scales with wave period and beach slope.

The relationship between ξ_0 and the distribution of runup was examined on a wider range of Iribarren space by Nielsen and Hanslow (1991). They found that the vertical scaling for runup distributions was proportional to ξ_0 for steep beaches, further supporting the original formulation of Hunt (1959), Eq. (4), and the empirical formulation of Holman (1986), Eq. (5). However, for beaches with $\beta<0.1$, they suggest that the dimensional vertical scaling of runup distributions may be independent of beach slope and proportional to $(H_0L_0)^{1/2}$ (Nielsen and Hanslow, 1991). The behavior of swash on a highly dissipative beach ($\xi_0<0.25$, $\beta<0.02$) was studied by Ruessink et al. (1998) who found that the swash signal was dominated by energy in the infragravity band (frequencies, f, <0.05 Hz) and scaled with H_0. Ruggiero et al. (2001) also studied runup under highly dissipative conditions and found that the elevation of R_2 scaled best with H_0.

Several studies have examined the relative roles of infragravity and incident ($f>0.05$ Hz) band swash (S_{IG} and S_{inc}, respectively) for particular field sites. Guza and Thornton (1982) showed that infragravity swash height increases linearly with offshore significant wave height, while energy in the incident band becomes saturated due to dissipation across the surf zone. This linear dependence of S_{IG} on H_0 has been confirmed by several other studies (Holman and Bowen, 1984; Howd et al., 1991; Raubenheimer and Guza, 1996); however, the constants of proportionality were found to vary between sites and with the wave and beach conditions present during each experiment. Howd et al. (1991) examined the relationship between infragravity motions at the shoreline and offshore wave height at a number of field sites and found their ratio to be dependent on ξ_0: larger constants of proportionality between infragravity motions and wave heights were observed on beaches with larger ξ_0 values. Ruessink et al. (1998) noted that the literature presents a wide range of constants of proportionality for the ratio S_{IG}/H_0, particularly between dissipative and reflective beaches, also suggesting that the ratio may depend on ξ_0.

Based on the previous studies described above, we propose the following general relationship for the elevation of extreme (2%) runup, R_2, for any data run:

$$R_2 = <\eta> + \frac{S}{2}, \text{ where} \tag{6}$$

$$S = \sqrt{(S_{inc})^2 + (S_{IG})^2}, \text{ and}$$
$$<\eta>,\ S_{inc},\ S_{IG} = f(H_0, T_0, \beta_f) \tag{7}$$

where T_0 is the deep-water wave period. The specific goal of this work is to improve the predictive equation for runup on

natural beaches by extending Holman's (1986) original analysis to data sets from 10 experiments representing a wide variety of beach and wave conditions and by separately parameterizing the individual runup processes: setup and swash.

In the next section, we describe our methods including details of the runup and swash statistics, the environmental parameters measures at each site, and the specific field experiments. Next, we present the results of our analysis, showing the parameterization of setup, incident swash, and infragravity swash, and evaluate the performance of the empirical parameterizations. The consequences of a longshore variable-topography on the parameterizations are also examined. In the Discussion section, the use of breaking wave height and surf-zone slope in the model, as alternatives to H_0 and β_f, is evaluated. Finally, improved parameterizations for setup and swash under dissipative conditions are presented.

3. Methods

3.1. Runup measurement technique and statistics

All runup data in this study were collected using video techniques that were developed at the Coastal Imaging Lab at Oregon State University and previously tested extensively against in situ runup instruments (Holland et al., 1995; Holman and Guza, 1984). Holman and Sallenger (1985) discussed difficulties with digitizing faint downwash, particularly on very low-sloping beaches. While variations in digitization can introduce noise in swash and setup statistics, Holman and Sallenger showed that they did so in a way that cancelled when runup peak elevations were found: slight lows in swash height were balanced by highs in set-up and visa versa. Other errors associated with video runup measurements are discussed in detail by Holman and Guza (1984) and Holland et al. (1995). The video pixel resolution, dependent on the field of view of the camera, the height of the camera, and the distance to the observed ground location (Holland et al., 1997), was typically 5–15 cm in the vertical with corresponding horizontal resolutions of 20–80 cm.

Cross-shore transects of pixel intensity (example from Duck, NC, Fig. 2a) were sampled at 1 or 2 Hz over 17- to 120-min record lengths, depending on the site. This created timestacks of pixel intensity on which runup and rundown can be seen as a white edge moving back and forth in the swash zone (Fig. 2b). The leading edge of runup was digitized from cross-shore timestacks of pixel intensity and then, using published photogrammetric relationships (Holland et al., 1997), was converted to time series of water level elevation measured relative to mean sea level. For each experiment, 17-min records were extracted from the longer time series to minimize the effects of changing tide levels on the location of wave breaking and on the area of the foreshore over which swash propagates. In order to calculate wave setup, measured tidal curves were removed from each time series. All statistics presented are representative of elevations measured relative to the still-water level.

Both continuous and discrete statistics were calculated from raw time series (Fig. 1a). After subtraction of the setup, $<\eta>$, the 17-min time average, swash statistics were calculated from the

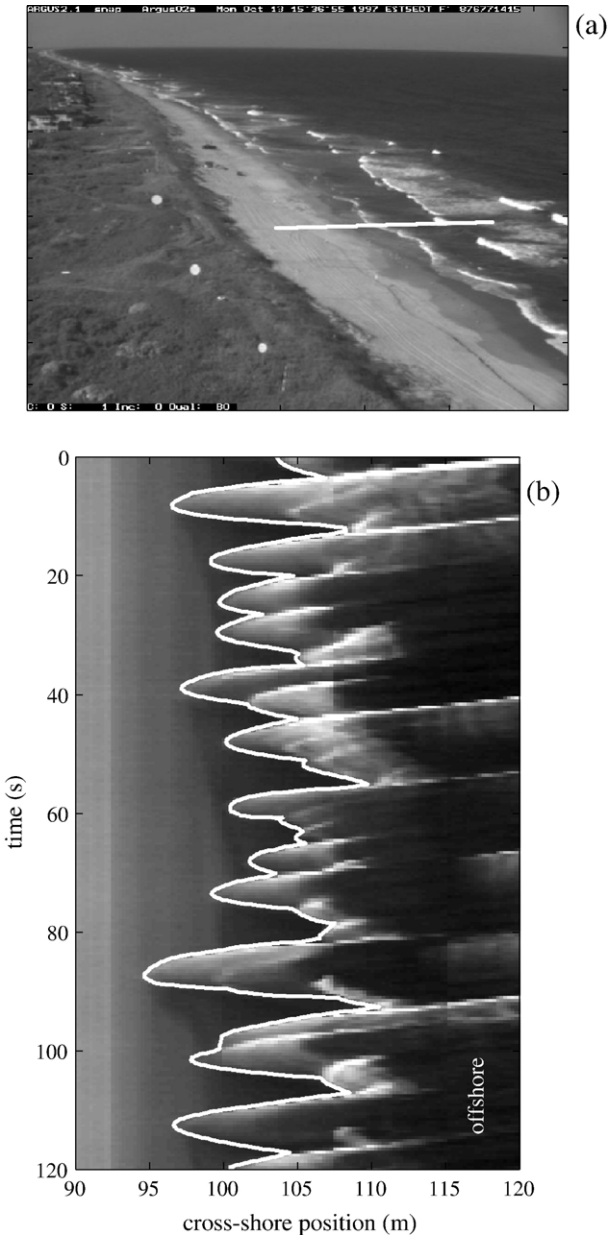

Fig. 2. Camera view from Duck, NC (a) and runup timestack (b). The cross-shore transect in (a) indicates the location of a single runup array. In the 120-s timestack of pixel intensity (b), each horizontal slice is the spatial variability of intensity at a single time step. The leading edge of swash is digitized through time (heavy, white line) and then converted into a time series of water-level elevations.

spectra, PSD(f), of the continuous water-level time series (Fig. 1b). The significant swash height, S, was calculated as,

$$S = 4^{*}\sqrt{\sum \mathrm{PSD}(f)\mathrm{d}f}, \tag{8}$$

similar to the calculation of significant wave height (Guza and Thornton, 1980). The significant swash in the incident (distinction based on wave frequency, $f>0.05$ Hz, and not on direction of propagation) and infragravity ($f<0.05$ Hz) bands were calculated by summing only over frequencies within the specified limits.

Runup statistics, R, were defined as the elevation of individual water-level maxima above the still-water level (Fig. 1a), merging contributions from setup and swash (Eq. (6)). The 2% exceedence value for runup, R_2, was calculated from the cumulative probability density function of runup elevations (Fig. 1c). This statistic, which represents the value of R that will be exceeded 2% of the time, is often used in engineering applications (Holman, 1986) and may be important for use in scaling the impacts of severe storms on beaches.

3.2. Environmental parameters

To make comparisons between sites where wave heights were measured in water depths varying between 7 and 20 m, an effective deep-water significant wave height, H_0, was calculated. To estimate H_0 during each water-level time series, measurements of significant wave height from local buoys and instrument arrays, H_s, were reverse shoaled to deep water using linear wave theory assuming a shore-normal approach. While this procedure neglects local generation, friction, white-capping, refraction, and diffraction, it allows for inter-comparisons of deep-water equivalent wave heights between different field sites. Breaking wave height, H_b, was calculated by shoaling H_s over local bathymetry using Thornton and Guza's (1983) wave transformation model, with the limiting ratio $\gamma = H_{rms}/h$ equal to 0.42 (Thornton and Guza, 1982) and the bore dissipation coefficient, B, equal to 1.0. While B was not tuned due to lack of appropriate field observations at each site, model error has been shown to be less than 10% when B is within 25% of its optimal value (Thornton and Guza, 1983). H_b was defined as the wave height occurring at the onset of wave breaking, identified as the seaward-most location where dissipation exceeded 20 W/m^2. Alternatively, the cross-shore location of breaking and H_b may be defined by the percent of waves breaking.

For each water-level time series, β_f was defined as the average slope over a region $\pm 2\sigma$ around $<\eta>$, where σ is the standard deviation of the continuous water level record, $\eta(t)$. Surf-zone slope, β_{sz}, is also considered here and was defined for each timestack as the slope between the shoreline (the cross-shore position of $<\eta>$), x_{sl}, and the cross-shore location of wave breaking, x_b. On barred profiles, the magnitude of β_{sz} may change significantly over the course of a day as the break point shifts from the sandbar at low tide toward the shoreline at high tide. These cases will be of special interest when trying to isolate the relative importance of foreshore and surf-zone slope.

3.3. Field experiments

Swash and runup data from 10 field experiments were compiled for this study: Duck, North Carolina, USA (1982, 1990, 1994, 1997); Scripps Beach, California, USA (1989); San Onofre, California, USA (1993); Terschelling, the Netherlands (1994, 1994); Gleneden, Oregon, USA (1994); and Agate Beach, Oregon, USA (1996). Table 1 provides details of experiment dates, mean wave and beach conditions (calculated over the durations of each experiment), as well as the number of runup measurements collected. The beach and wave conditions during these experiments represent a full range of ξ_0 with Terschelling and Agate Beach representing the dissipative end ($\xi_0 < 0.3$) and San Onofre representing the most reflective conditions ($\overline{\xi_0} = 2.2$). Mean beach profiles, averaged over the duration of each experiment, illustrate the differences in beach slope and offshore bathymetry (Fig. 3).

Table 1
Average environmental conditions for each experiment

Site	Date	$\overline{H_s}(m)$	$\overline{T_0}(s)$	$\overline{\beta_f}$	$\overline{\xi_0} \pm \sigma$	N (N_{single})
Duck, NC (Duck82)	5–25 Oct 1982	1.7	12.0	0.11	1.4±0.5	149 (36)
Scripps Beach, CA	26–29 Jun 1989	0.7	10.0	0.04	0.6±0.1	42 (41)
Duck, NC (Delilah)	6–19 Oct 1990	1.5	8.9	0.10	0.9±0.4	1829 (138)
San Onofre, CA	16–20 Oct 1993	0.8	14.9	0.10	2.2±0.3	59 (59)
Gleneden, OR	26–28 Feb 1994	2.1	12.4	0.08	0.9±0.2	52 (42)
Terschelling, NL	2–22 Apr 1994	2.4	8.0	0.02	0.1±0.04	41 (6)
Terschelling, NL	1–21 Oct 1994	1.4	8.1	0.01	0.1±0.05	27 (8)
Duck, NC (Duck94)	3–21 Oct 1994	1.5	12.1	0.08	1.1±0.3	975 (52)
Agate Beach, OR	11–17 Feb 1996	2.5	13.2	0.02	0.2±0.05	126 (14)
Duck, NC (SandyDuck)	3–30 Oct 1997	1.3	9.5	0.10	1.2±0.7	491 (95)

$\xi_0 \pm \sigma$ — mean Iribarren number ± the standard deviation.
N — number of individual estimates of runup statistics, includes multiple longshore lines.
N_{single} — number of individual estimates of runup statistics used in bulk parameterization.

The bulk of the data (91%) was collected at the U.S. Army Corps of Engineers Field Research Facility (FRF) in Duck, NC, and represents intermediate to reflective conditions (as defined by Wright and Short (1983), $0.3 < \xi_0 < 4.0$). The typical profile here is characterized by an offshore sandbar and a mean foreshore slope of 0.1. H_s and T_0 were recorded hourly at a Waverider buoy located in ~18 m of water. Tide level was measured every 6 min at a NOAA tide gauge mounted at the end of the FRF pier. Bathymetry was sampled roughly daily during the Duck experiments in 1990, 1994, and 1997 and every few days during the 1982 experiment using the Coastal Research Amphibious Buggy (Birkemeier and Mason, 1984). Additional high-resolution foreshore topographic surveys were usually collected daily during all experiments. During Duck82 (1982), runup was digitized from 35-min time-lapse photography along selected longshore locations (Holman, 1986) following methods outlined in Holman and Guza (1984), resulting in 149 estimates of runup and swash statistics. The runup array during the Delilah experiment (1990) consisted of 26 longshore lines with a longshore spacing, dy, of 10 m, sampled at 2 Hz (Holland and Holman, 1993). During the Duck94 experiment (1994), 120-min runup timestacks were collected at up to 48 equally spaced (dy = 5 m) cross-shore lines (Holland and Holman, 1996). The runup array from SandyDuck (1997) consisted of five cross-shore transects from

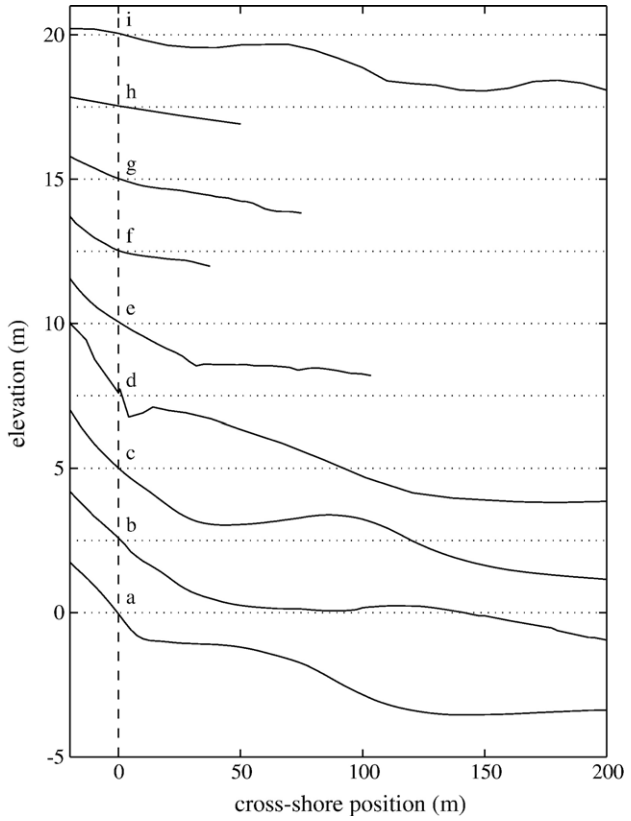

Fig. 3. Time-averaged profile (topography and bathymetry) from each experiment illustrating differences in foreshore slope and offshore profiles: SandyDuck (a), Duck94 (b), Delilah (c), Duck82 (d), San Onofre (e), Gleneden (f), Scripps Beach (g), Agate Beach (h), and Terschelling (i). The profiles are offset 2.5 m in the vertical. Mean sea level is indicated by the horizontal dotted lines. The vertical dashed line marks the cross-shore location of MSL for each profile ($x=0$). The average profile was calculated over the time period of the experiment at a single cross-shore transect.

which approximately 500 17-min swash timestacks were collected.

More limited data exist from three other intermediate/reflective sites. The Uswash experiment was conducted June 26–29, 1989 at Scripps Beach, CA, a fine-grained sandy beach (Holland et al., 1995). Offshore bathymetry was not measured on a daily basis and was approximated offshore of the 1-m depth contour using an offshore slope of 0.01 (Holland et al., 1995). Wave height and period were measured every 6 h in 7 m water depth, a few hundred meters offshore, as a part of the Coastal Data Information Program (CDIP) (Seymour et al., 1985). Six 8-Hz data runs were collected over the course of the experiment (Holland et al., 1995). A more reflective data set was collected during a October 1993 experiment in San Onofre, CA. The offshore slope was measured to be 0.013 from a cross-shore profile, surveyed early in the experiment (October 10, 1993), that extended approximately 100 m offshore. Wave data were obtained from a CDIP buoy located offshore of Oceanside, CA, in approximately 10 m of water, a few kilometers southeast of the field site. Tide measurements were obtained from a NOAA gauge located in La Jolla, CA. 120-min timestacks of runup were collected at 2 Hz at a single cross-shore transect over a 5-day period. The final data set on an intermediate beach was obtained from an experiment at Gleneden, OR, in late February 1994. A linear offshore profile ($\beta=0.025$) was extrapolated from a survey that extended from the beach across the surf zone. Incident wave conditions were measured at a CDIP buoy located approximately 190 km to the southeast in 11 m of water. Tides measured at Yaquina Bay, OR, located 35 km to the south, were corrected so that the values were representative of the tides at Gleneden. 120-min video runup timestacks were collected at 2 Hz multiple times a day along a single cross-shore transect.

Data from two beaches dominated by dissipative conditions ($\xi_0<0.3$) are also included in the data set, providing a small (5.3% of the total data) but important extension into highly dissipative domains. Two data sets were collected from Terschelling, the Netherlands, in April and October 1994 by Ruessink et al. (1998). Terschelling features multiple offshore sandbars with offshore slopes generally 0.005 or less, as measured from a single offshore bathymetry profile. Daily beach surveys were conducted and an alongshore-averaged foreshore slope was calculated for the analysis of runup statistics at seven cross-shore transects (Ruessink et al., 1998). H_s, as measured by an offshore buoy located approximately 5 km offshore in 15 m water depth, ranged from 0.5 m to almost 4 m. 45-min runup timestacks were collected at 2 Hz along nine cross-shore lines once a day. Because the only beach slope available for this site was an alongshore-averaged foreshore slope, the runup and swash statistics computed at each cross-shore line were alongshore averaged before being compared in bulk to the other sites. (Runup statistics were fairly longshore uniform during each data run. Over the duration of the experiment, the mean and standard deviation, $\mu\pm\sigma$, of longshore-variable swash and setup were 69 ± 8 and 16 ± 5 cm, respectively.) The second dissipative site is Agate Beach, OR, a multiple-barred, low-sloping beach where runup data were collected in February 1996 as a part of a larger experiment on the nearshore dynamics of high-energy beaches (Ruggiero et al., 2001). Foreshore slopes were measured daily using GPS topographic surveys. Offshore survey data were not available for this experiment; however, a typical offshore slope was measured from surveys collected in 1998 to be ~0.01. Wave height and period were obtained from a CDIP buoy located approximately 170 km to the southeast in 64 m water depth. Measured tides were taken from a NOAA gauge located at Yaquina Bay, OR, approximately 8 km from Agate Beach. 120-min runup timestacks were collected at 1 Hz at five cross-shore transects.

4. Results

For the initial analysis of bulk runup statistics, the complications of longshore variability were avoided by selecting a single cross-shore transect from each experiment. Limiting the data to one runup line per experiment also helped to minimize the bias towards intermediate conditions since the most extensive longshore coverage occurred during the Duck experiments. This resulted in 491 independent measures of runup and swash, distributed as follows: Duck82 (36), Uswash (41), Delilah (138), San Onofre (59), Terschelling (14), Gleneden (42), Duck94 (52), Agate Beach (14), and SandyDuck (95). The statistics of longshore variability from multiple-transect runs are examined later in the paper.

The assumption that the 2% exceedence level for runup approximately equals $<\eta>+S/2$ (Eq. (6)) was first tested. S is calculated as four times the square root of the swash variance (4σ) and, for a Gaussian process, would encompass 95.4% of the values. The remaining 4.6% defines the extreme high and low values and is split evenly between the tails of the distribution. Accordingly, the actual value of the extreme low value of runup (the 98% exceedence value) would be defined as the mean (setup) minus half of the spread (2σ, or $S/2$), and the extreme high value of runup (the 2% exceedence value) would be defined as the mean (setup) plus half of the spread. The squared-correlation between the measured values of $<\eta>+S/2$ and R_2 is 0.94, which is significant at the 99% confidence level (Fig. 4). The slope of the regression is 1.1, which reflects the slightly non-Gaussian nature of natural swash. To test whether the observed swash was Gaussian, the skewness and kurtosis of each swash distribution were calculated for all experiments, except Duck82, and compared to values defining Gaussian distributions (skewness=0, kurtosis=3). The mean kurtosis for all data was 2.9 ($\sigma=0.80$). The mean skewness for all swash distributions was 0.19 ($\sigma=0.38$) indicating that natural swash is slightly skewed. To account for this skewness, the slope of the regression in Fig. 4 is included in Eq. (6), resulting in a more complete definition of runup,

$$R_2 = 1.1 \cdot \left[<\eta> + \frac{S}{2} \right]. \tag{9}$$

The empirical models described in the following sections will be presented in dimensional space and based on regressions forced through the origin. Synthetic tests based on samples with known statistical characteristics indicate a danger in carrying out the least-squares analysis in non-dimensional space, as has been common in the literature. In a regression between non-dimensional R_2 (normalized by H_0) and ξ_0, it is found that small errors in data from small wave cases will map to large errors in ξ_0 and can introduce large errors in regression statistics. Thus, in order to avoid undue influence of these errors and to better weigh storm events, the dimensional parameterization is preferable to its non-dimensional counterpart. Regressions through the origin are used, rather than allowing least squares intercepts, in order to avoid non-physical results in setup and swash models. For example, a significant intercept in a relationship between wave height normalized swash and ξ_0 would results in a value of swash when $H_0=0$. In most models presented here, the computed intercept was not significantly different than zero, supporting the selection of regression through the origin methodology. To evaluate each empirical model, the squared-correlation, ρ^2, referred to hereafter simply as correlation, and the 95% significance level, ρ^2_{sig}, are presented as a measure of the linear relationship between the two parameters. The goodness of fit of the empirical model is measured using an rms error, rmse.

4.1. Setup

No single constant of proportionality between $<\eta>$ and H_0 was found ($\rho^2=0.30$, rmse=25.3 cm; Fig. 5a). The setup parameterization was improved by inclusion of L_0 (T_0) and β_f (Fig. 5b), modeling setup using a dimensional, Iribarren-like form ($\xi_0 H_0$),

$$<\eta> = 0.35\beta_f (H_0 L_0)^{1/2}. \tag{10}$$

The squared-correlation of the dimensional model is $\rho^2=0.48$ ($\rho^2_{sig}=0.01$) and rmse=21.3 cm. A summary of the regression coefficients, squared-correlations, and rms error for all suggested parameterizations is presented in Table 2.

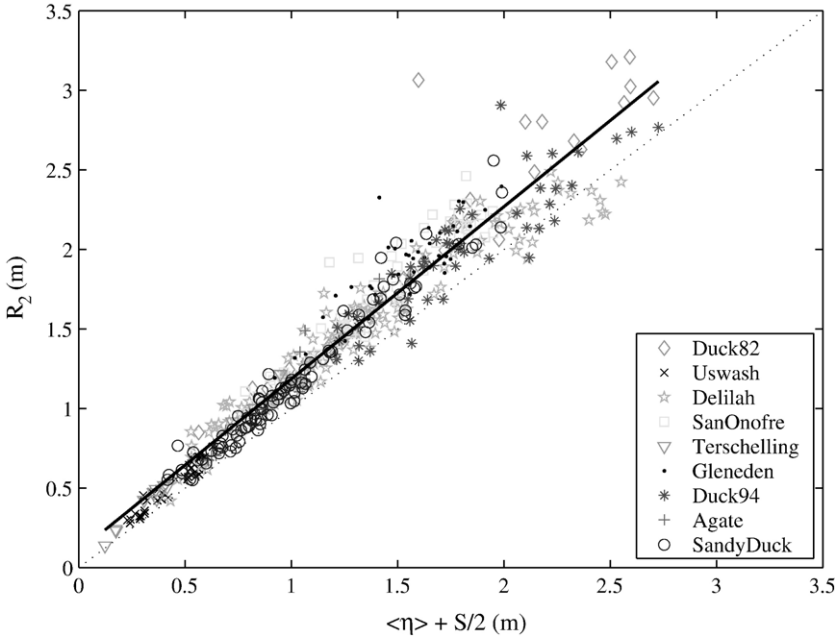

Fig. 4. The sum of setup and half of the swash excursion plotted against the 2% runup peak elevation. The dashed line is a 1 : 1 line. The heavy solid line is the best fit to the data ($m=1.1$, $b=0.10$, $\rho^2=0.94$).

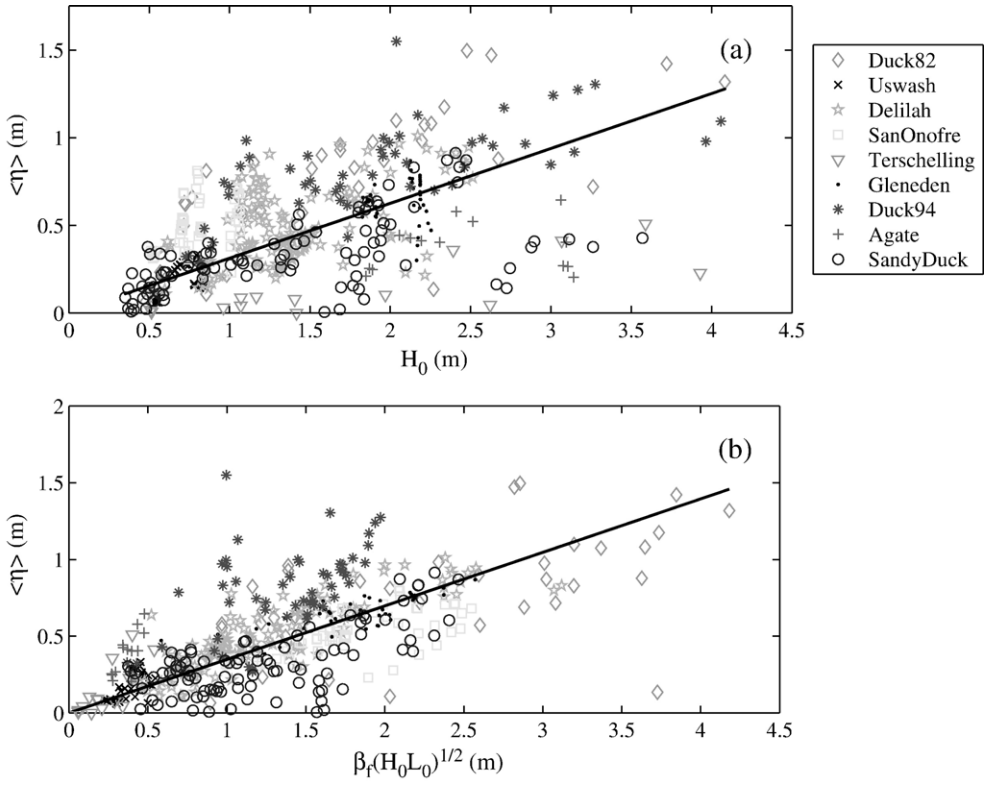

Fig. 5. (a) Setup vs. wave height ($\rho^2=0.30$) and (b) setup vs. $\beta_f(H_0L_0)^{1/2}$ ($\rho^2=0.48$). The $\beta_f(H_0L_0)^{1/2}$ dimensional parameterization also has the lowest rms error, 21.3 cm.

Setup data were divided into low-, mid-, and high-tide groupings with divisions defined as 1/3 (low to mid) and 2/3 (mid to high) of the tidal range observed at each site. As was observed in the Duck82 data by Holman and Sallenger (1985), the goodness of fit of the parameterization for $<\eta>$ varied during different stages of the tide (Fig. 6). When low-tide values of $<\eta>$ were examined separately from those occurring during mid- and high tide, the correlation between $<\eta>$ and $\beta_f(H_0L_0)^{1/2}$ fell to $\rho^2=0.29$ (Fig. 6a). For the mid- and high-tide values, the correlation remained high, $\rho^2=0.52$ (Fig. 6b). It was suggested by Holman and Sallenger (1985) that offshore morphology and surf-zone slope play a larger role in $<\eta>$ at low tide, with breaking patterns over barred topographies producing more complex patterns in radiation stress gradients (Raubenheimer et al., 2001). However, the use of surf-zone slope in any form of a setup parameterization for the low-tide data did not improve the model performance over the β_f-dependent parameterization (Eq. (10)) that was derived from the data set as a whole.

Table 2
Regression parameters for components of runup model

	Quantity modeled	Model input	Slope, m	Intercept, b [a]	ρ^2 (ρ^2_{sig})	rmse (cm)
All sites	$<\eta>$	$\beta_f(H_0L_0)^{1/2}$	0.35 (±0.01)	0	0.48 (0.01)	21.3
	S_{inc}	$\beta_f(H_0L_0)^{1/2}$	0.75 (±0.03)	0	0.44 (0.01)	46.9
	S_{IG}	$(H_0L_0)^{1/2}$	0.06 (±0.002)	0	0.65 (0.01)	25.7
$\xi_0<0.3$	$<\eta>$	$(H_0L_0)^{1/2}$	0.016 (±0.003)	0	0.68 (0.22)	11.9
	S	$(H_0L_0)^{1/2}$	0.046 (±0.004)	0	0.78 (0.22)	15.7

[a] Regressions forced through origin to avoid non-physical intercepts.

4.2. Incident and infragravity swash

On dynamically different beaches, energy in the incident and infragravity frequency bands will contribute varying amounts to total swash (Guza and Thornton, 1982). Swash heights within these two bands are forced by different processes and therefore require separate parameterizations. Incident swash is best parameterized by a dimensional version of an Iribarren-like relationship (Fig. 7a),

$$S_{inc} = 0.75\beta(H_0L_0)^{1/2}. \quad (11)$$

The correlation for the model is $\rho^2=0.44$ ($\rho^2_{sig}=0.01$) and rmse=46.9 cm, lower than that for the non-dimensional version.

When the same dimensional model is used to describe the infragravity band (Fig. 7b), the correlation remains high, $\rho^2=0.56$ (rmse=34.2 cm). However, when local foreshore slope is removed from the expression (Fig. 7c), the correlation improves to $\rho^2=0.65$ ($\rho^2_{sig}=0.01$) and the rms error decreases to 25.7 cm. The magnitude of infragravity swash is, therefore, linearly independent of β_f and best parameterized as

$$S_{IG} = 0.06(H_0L_0)^{1/2}. \quad (12)$$

The absence of beach slope in this model may be somewhat counter-intuitive given that the presence of

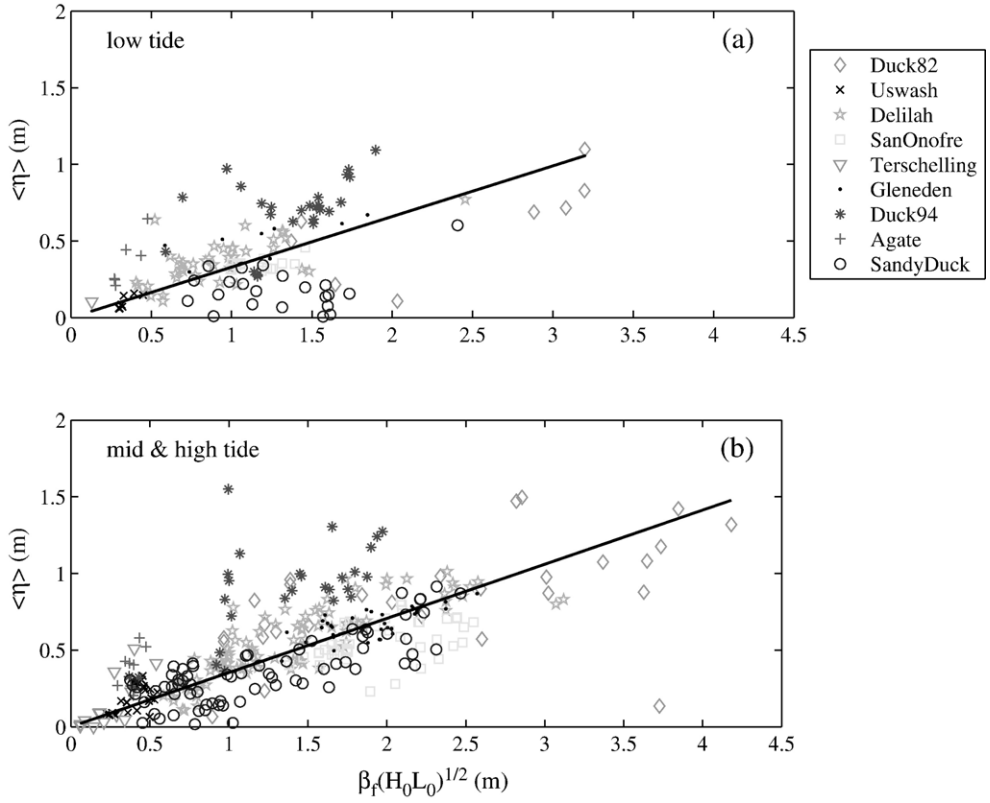

Fig. 6. Setup vs. $\beta_f(H_0L_0)^{1/2}$ during low tide (a) and mid- and high tide (b). The correlation of the model during low tide ($\rho^2=0.29$) is significantly lower than that for mid- and high-tide values ($\rho^2=0.52$).

significant infragravity band energy is prescribed by the β-dependent ξ_0. However, the inclusion of β_f in the parameterization of the actual magnitudes of S_{IG} has not been supported by our observations. The non-dimensional form of Eq. (12) shows that the efficiency of infragravity energy generation is inversely dependent on deep-water wave steepness, H_0/L_0, where low values are indicative of swell conditions (for a given value of H_0). Infragravity band motions have previously been shown to correlate best with energy from swells rather than that from seas (Elgar et al., 1992).

4.3. Evaluation of swash and runup parameterization

Estimated setup, $\langle\eta\rangle_e$, swash, S_e, and runup peaks, R_{2e}, were calculated from measured offshore wave height, wave period, and foreshore beach slope using the empirical parameterizations for setup, incident swash, and infragravity swash (Eqs. (10)–(12)) in Eq. (9). Performance of the parameterizations was measured in terms of dimensional differences, Δ, from observations,

$$\Delta\langle\eta\rangle(t) = \langle\eta\rangle_e(t) - \langle\eta\rangle(t), \tag{13}$$

$$\Delta S(t) = S_e(t) - S(t), \text{ and} \tag{14}$$

$$\Delta R(t) = R_{2e}(t) - R_2(t) \tag{15}$$

where $\langle\eta\rangle(t)$, $S(t)$, and $R_2(t)$ are the observed values at each time, t. The mean difference errors, $\overline{\Delta}$, were calculated for each experiment and for all data as a measure of the bias of the estimator. The rms error of the differences, Δ_{rms}, was used to measure the scatter or noise of the estimate. Mean values for observed setup, swash, and runup ($\overline{\langle\eta\rangle}$, $\overline{S}$, and $\overline{R}$ respectively) are presented in order to evaluate the significance (or relative magnitudes) of the mean difference errors. Summaries of the error statistics are presented in Table 3.

The mean error between setup estimates and observations, averaged over all experiments, $\overline{\Delta\langle\eta\rangle}$, is −3 cm, while the rms error, $\Delta\langle\eta\rangle_{rms}$, is 21 cm ($\overline{\langle\eta\rangle}=49$ cm). There is little bias in setup estimates on intermediate and reflective beaches ($\overline{\Delta\langle\eta\rangle}=2$ cm, $\overline{\langle\eta\rangle}=57$ cm); however, on dissipative beaches ($\xi_0<0.3$), the bulk parameterization underestimates setup elevation by 16 cm ($\overline{\langle\eta\rangle}=27$ cm). Accordingly, the largest underestimates of setup occur for large wave events ($H_0>1.5$ m, $\overline{\Delta\langle\eta\rangle}=-7$ cm) and on the most gentle beach slopes ($\beta_f\leq 0.02$, $\overline{\Delta\langle\eta\rangle}=-17$ cm).

The mean difference in swash, $\overline{\Delta S}$, averaged over all data, is 34 cm and the rms difference, ΔS_{rms}, is 46 cm ($\overline{S}=149$ cm). The bulk parameterization for runup contains an −18 cm bias ($\overline{R}=144$ cm). The rms difference error between runup estimates and observations, $(\Delta R)_{rms}$, is 38 cm. The bias in the runup measurements is two times larger on intermediate and reflective beaches ($\overline{\Delta R}=-18$ cm) than on dissipative sites ($\overline{\Delta R}=-9$ cm); however the observed runup magnitudes are also larger on intermediate and reflective sites ($\overline{R}=148$ cm) than dissipative ones ($\overline{R}=84$ cm).

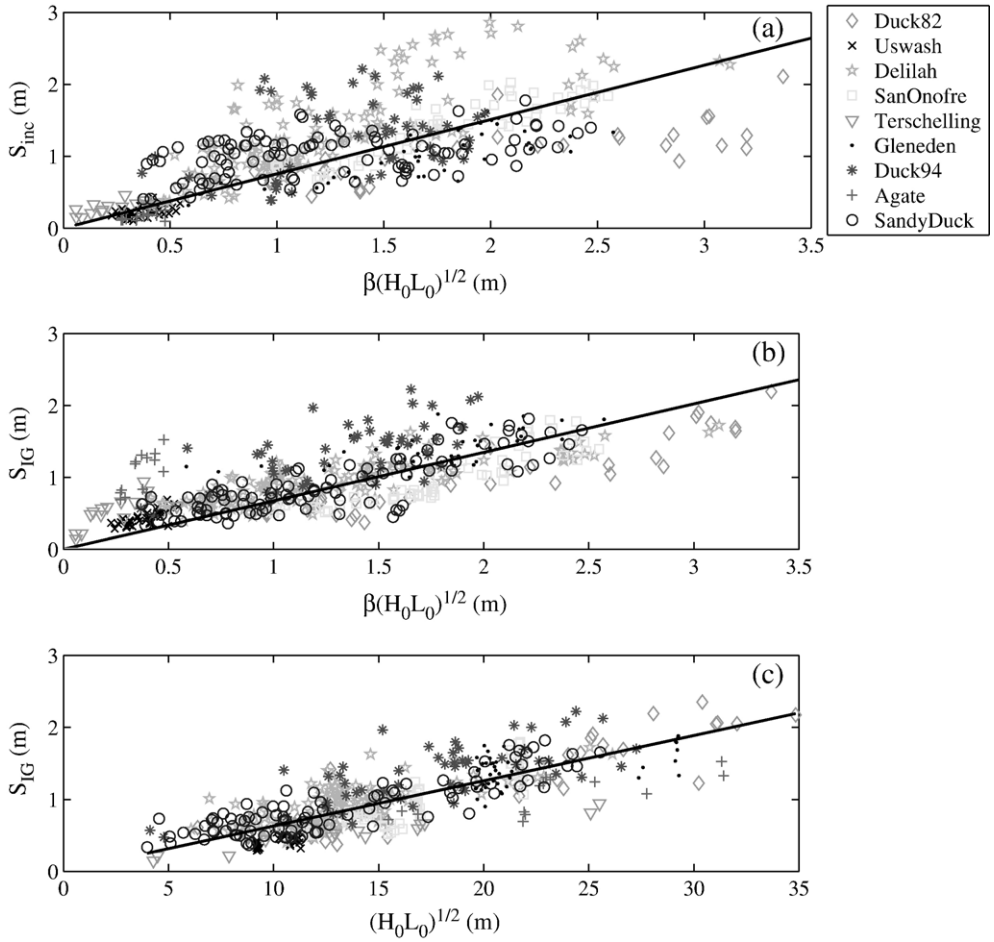

Fig. 7. (a) Incident (ρ^2=0.44, rmse=46.9 cm) and (b) infragravity swash (ρ^2=0.56, rmse=34.2 cm) parameterized in a dimensional form of the traditional Iribarren-based equation. (c) The parameterization of infragravity swash improves when beach slope is removed from the model (ρ^2=0.65, rmse=25.7 cm).

4.4. Longshore variability

Runup and incident swash have been shown to be dependent on foreshore beach slope. Accordingly, beaches with significant longshore-variable slopes should exhibit similar longshore variability in swash excursions and runup elevation. However, since S_{IG} showed little or no linear dependence on β_f, spatial variations in the infragravity band swash are expected to be less than those in the incident band. To explore the dependencies on beach slope, the longshore variability of swash and runup was examined using longshore runup arrays from the Delilah (26 lines; total array length, Y, =250 m), Duck94 (35 lines; Y=165 m), and SandyDuck (6 lines; Y=75 m) experiments. Spatial variability observed at each site was characterized by calculating the longshore standard deviation of the total swash excursions, $\sigma S(t)$, as well as that of the incident, $\sigma S_{inc}(t)$, and infragravity, $\sigma S_{IG}(t)$, components. Additionally, spatial squared-correlations, ρ_s^2, were calculated between $S(y)$, $S_{inc}(y)$, $S_{IG}(y)$ and $\beta_f(y)$ in

Table 3
Accuracy of setup, swash, and runup parameterizations, given in (cm)

Experiment	$\overline{\Delta<\eta>}$	$\Delta<\eta>_{rms}$	$\overline{\Delta S}$	ΔS_{rms}	$\overline{\Delta R}$	ΔR_{rms}
Duck82	3	34	48	58	9	37
Scripps Beach	−5	9	18	19	2	10
Delilah	−6	13	42	57	−32	41
San Onofre	11	16	17	22	−4	17
Gleneden	−2	9	20	27	−17	27
Terschelling [a]	−6	14	25	31	−1	13
Duck94	−33	40	54	67	−62	69
Agate Beach	−25	28	34	39	−16	27
SandyDuck	11	20	31	37	−2	34
Average error, all data	−3	21	34	46	−18	38
	$\overline{<\eta>}$ = 49 cm		$\overline{S}$ = 149 cm		$\overline{R}$ = 144 cm	

Mean observed values of setup, swash, and runup are presented in the last row in order to examine mean error magnitudes relative to observed values.

[a] The results of the two Terschelling field campaigns are combined in these statistics.

Table 4
Longshore variability of swash and correlations to foreshore beach slope

Experiment	σS (m)	σS_{inc} (m)	σS_{IG} (m)	$\%\rho_s^2(S,\beta_f)$ significant ($\%\rho_s>0$)	$\%\rho_s^2(S_{inc},\beta_f)$ significant ($\%\rho_s>0$)	$\%\rho_s^2(S_{IG},\beta_f)$ significant ($\%\rho_s>0$)
Delilah	0.24	0.23	0.15	45.8 (97.0)	50.0 (100)	13.9 (80.0)
Duck94	0.20	0.24	0.19	31.0 (77.8)	55.2 (100)	38.0 (0)
SandyDuck	0.18	0.18	0.14	55.6 (100)	58.6 (100)	14.8 (100)

The first three columns indicate the spatial standard deviation of swash. The last three columns list the percentage of spatial correlations significant at the 95% confidence level. The value in parenthesis indicates the percentage of significant correlations that are positive.

order to determine the amount of longshore variability in swash that may be attributed to a longshore-variable foreshore slope. Table 4 presents the details of longshore variability (the standard deviation of S, S_{inc}, and S_{IG}) and the correlation analysis (the percentage of significant correlations and of positive significant correlations) for each of the three experiments considered.

At Delilah and SandyDuck, the total swash excursion was most longshore variable on days when the beach topography was highly three dimensional, either in the form of a regular cusp field, a large megacusp embayment, or welded swash bars (σS=40–50 cm). The values of $\rho_s^2(S,\beta_f)$ showed a positive correlation between total swash and beach slope, indicating that increases in S corresponded to increases in β_f, consistent with expectations. Correlations were significant at the 95% confidence level 46% (Delilah) and 56% (SandyDuck) of the time (Table 4). Correlation values were higher and more often significant for rhythmic, large-scale spatial variations in slope (i.e., megacusps) than for irregular, short-scale slope variations. The time-averaged value of σS_{inc} was higher than σS_{IG}, indicating that most of the observed longshore variability in total swash was contained within the incident band. Additionally, S_{inc} was significantly and positively spatially correlated to β_f for 50% and 59% of the cases at Delilah and SandyDuck, respectively (Table 4). Less variability was observed in S_{IG} and correlations with β_f were significant only 15% of the time (Table 4), supporting the results that the magnitude of infragravity swash has little or no linear dependence on foreshore beach slope.

During Duck94, when a well-developed cusp field was present, there was less of a relationship between the magnitude of the longshore variability observed in total swash and that observed in beach slope. Spatial correlations between S and β_f were significant only 31% of the time. Correlations between S_{inc} and β_f were significant and positive 55% of the time. When the cusp field was particularly well-developed, longshore variability within the infragravity band increased. Significant correlations between S_{IG} and β_f were more than twice as common during Duck94 than during the other experiments (Table 4). Surprisingly, significant values of $\rho_s^2(S_{IG},\beta_f)$ were always negative, indicating that S_{inc} and S_{IG} were out of phase within the cusp field. This relationship between S_{IG}, S_{inc}, and beach slope may be related to longshore-variable dynamics due to swash circulation within a cusp field, as opposed to a simple cross-shore flow which has been assumed for the empirical parameterizations presented. An exploration of the longshore variability of setup, swash, and runup and the complex dynamics of incident and infragravity swash, particularly on highly three-dimensional topography, will be presented in detail in a subsequent paper.

The dependence of total swash on β_f will have implications on the practical use of the bulk parameterization of runup on beaches with complex foreshore topography. In order to evaluate how much error can be expected in estimates of R_2 if a longshore-averaged slope, $\overline{\beta_f}$, is used instead of a more accurate measure of slope at each longshore line, $\beta_f(y)$, a relative slope difference was compared to a relative runup error. Relative slope difference, $\delta\beta$, was defined as $(\overline{\beta_f}-\beta_f(y))/\beta_f(y)$. Relative error in runup elevation, δR_2, was defined as $(R_{2avg}-R_{2e}(y))/R_{2e}(y)$, where R_{2avg} is the estimate of runup calculated from a single longshore-averaged beach slope and $R_{2e}(y)$ is the runup calculated using $\beta_f(y)$ measured at each longshore line. The error in a runup estimate calculated from a single longshore-averaged beach slope was found to equal 51% of $\delta\beta$. For example, a 20% difference between $\overline{\beta_f}$ and $\beta_f(y)$ would result in a 10.2% error in estimated runup. Maximum alongshore variability of β_f was observed during the Delilah experiment when megacusps were present (longshore spacing of ~200 m, $\delta\beta$=−0.25 to 0.75). Here, runup predictions based on a longshore-averaged beach slope may be underestimated by 12% on foreshore locations that are more steeply sloped than $\overline{\beta_f}$ and overestimated by as much as 38% on more gently sloped regions. On a well-developed cusp field, longshore variability in foreshore slope ($\delta\beta$=−0.3 to 0.5) may result in runup values 15% lower than the true value on steep cusp horns and overestimates of 26% within the more gently sloped cusp embayments. Again, swash circulation within a cusp field may be affecting the observed runup amplitudes, partly explaining why a change in beach slope leads to a 51% change in runup, even though the parameterizations show a linear relationship between the two.

5. Discussion

The proper choice of wave height in the parameterization of total swash, S, was explored as a part of this study. The most rigorous comparison between H_s (a locally measured significant wave height), H_0 (deep-water equivalent wave height), and H_b (breaking wave height) could be completed for the Duck experiments because accurate, daily bathymetry data were available for shoaling the waves and determining an approximate break point. At this site, the dimensional Iribarren-based parameterization for S calculated using H_b (ρ^2=0.46, rmse=57.9 cm) showed no improvement over the similar swash parameterization calculated using H_0 (ρ^2=0.46, rmse=56.4 cm). On the dissipative beaches, where daily offshore bathymetry data were not available, an approximation of H_b was made by shoaling H_s over the single offshore profile available for each site. On these beaches, H_b was found to improve the performance of the regression: the correlation was higher, ρ^2=0.80 (ρ_{sig}^2=0.22) than that for the swash parameterization based on H_0 (ρ^2=0.67). However, because daily profiles were not measured at these sites and the values of H_b are approximate, the exact relationship between H_b and S cannot be clearly defined here.

While H_b was not shown to offer a significant improvement over H_0 (at Duck), the question of which measure of wave height is most appropriate for practical use in runup parameterizations remains a relevant one. Because of refraction, frictional dissipation across the shelf (Herbers et al., 2000), and white-capping, the wave height measured at a buoy located in deep water may be significantly higher than that which actually reaches the nearshore, so runup predictions using deep-water buoy measurements may be anomalously high. Analysis at Duck, where wave height measurements are available in deep water, 18 m water depth, and 8 m water depth, shows a somewhat

stronger relationship between runup and waves measured at 8 m. While H_0 was used in this analysis as an equal measure of wave height between different sites, in practical applications, it may be preferable to use local wave measurement, reverse shoaled to an equivalent deep-water value.

Some researchers have suggested that the slope of the surf zone (β_{sz}) might be more directly related to swash height than β_f; therefore, its use in the empirical parameterization would likely improve runup estimates (Holman and Sallenger, 1985; Nielsen and Hanslow, 1991). To test this idea, β_{sz} was substituted in the dimensional, Iribarren-based parameterization for total S. When the entire data set was used, the correlation of the model ($\rho^2=0.03$, $\rho^2_{sig}=0.01$) decreased significantly from the similar model calculated using β_f ($\rho^2=0.68$, $\rho^2_{sig}=0.01$). The data from Delilah, Duck94, and SandyDuck were examined separately because the detailed, daily bathymetric surveys provided more accurate estimates of β_{sz}. Here, the correlation for the model for S using β_{sz} was not significantly different than zero showing that, on these beaches, the foreshore slope has more of an influence on swash processes than the surf-zone slope. When dissipative beaches were isolated from the entire data set and examined separately, the use of estimated β_{sz} showed similar predictive capabilities ($\rho^2=0.71$, rmse=20.1 cm) as calculations based on β_f ($\rho^2=0.67$, rmse=21.3 cm). However, the correlation of the model for swash on dissipative beaches is highest when slope is completely removed from the parameterization ($S\propto(H_0L_0)^{1/2}$, $\rho^2=0.78$). In order to explore the effects of β_{sz} on runup more directly, the variations in S were studied as the tide rose and fell over a barred profile at Duck. Since β_{sz} is defined between the shoreline and the break point (x_b), a significant change in β_{sz} is observed under certain wave conditions where breaking occurs on the bar at low tide (gentle β_{sz}) and near the shoreline at high tide (steep β_{sz}). Data runs where these conditions were met were isolated from the larger data set. This unique situation allows for a changing surf-zone slope while the input wave conditions remain relatively constant. On most topographies observed, the magnitude of runup and swash did not change dramatically over the change in tide or related changes in x_b. Both R_2 and S correlated well with β_f over the entire tidal cycle. (See Section for 4.4 for detailed correlations between S and β_f.) These results again indicate that β_{sz} offers no significant improvement over β_f for incident-band-dominated sites. (Note: Variability in the magnitude of S_{inc} was observed over a few tidal cycles at Duck94 when beach cusps were present on the foreshore, perhaps related to the complex interactions between incident and infragravity band swash on this rhythmic topography.)

While the goal of this work was to present a parameterization for extreme runup that is useful and accurate on a broad spectrum of beaches, it is important to address the errors that occur during dissipative conditions ($\xi_0<0.3$) when R_2 is estimated using the bulk parameterization (Eqs. (10)–(12)). Under these extreme end-member conditions, increased dissipation likely becomes a significant term in momentum balances and the parameterization from steeper conditions no longer works. When the dissipative beaches are isolated from the whole data set, the correlation of the parameterization of setup improves ($\rho^2=0.67$). Interestingly, when β_f is removed from the parameterization of setup for dissipative conditions, there is no decrease in the correlation of the model. This suggests that the inclusion of β_f in this parameterization is not necessary, supporting earlier work which found that shoreline setup on dissipative beaches was not linearly dependent on beach slope

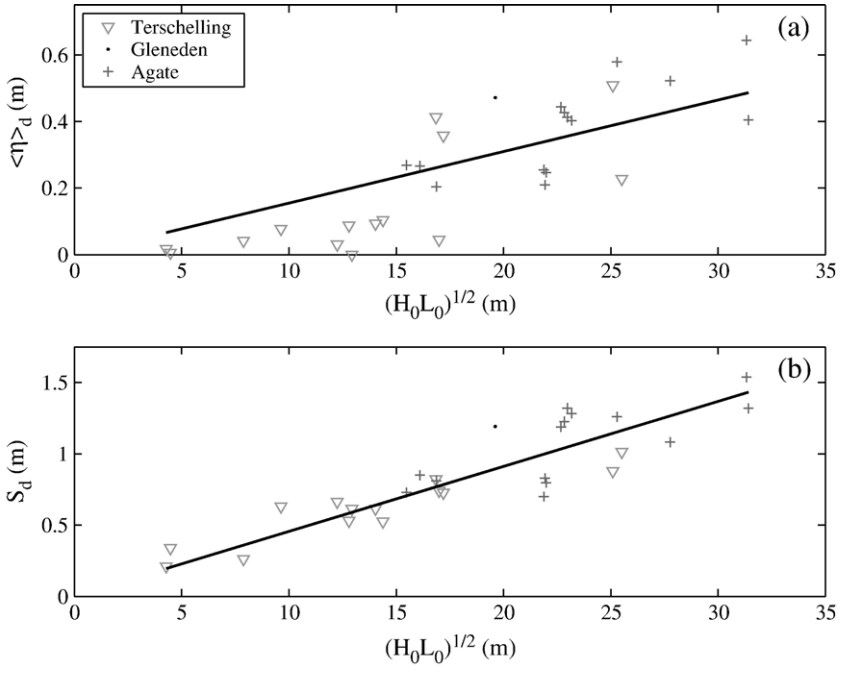

Fig. 8. Parameterization of (a) setup ($\rho^2=0.68$, rmse=11.9 cm) and (b) swash ($\rho^2=0.78$, rmse=15.7 cm) during dissipative conditions only ($\xi_0<0.3$) using $(H_0L_0)^{1/2}$. For both models, the correlations are equal or higher than when the bulk parameterizations are used for the dissipative conditions subset.

(Hanslow and Nielsen, 1993). The suggested parameterization for setup on dissipative sites, $<\eta>_d$ (Fig. 8a), is

$$<\eta>_d = 0.016(H_0L_0)^{1/2} \quad (16)$$

($\rho^2=0.68$, $\rho^2_{sig}=0.22$, rmse=11.9 cm). On dissipative beaches, frictional dissipation of large waves over extremely wide, low-sloping surf zones begins to play a larger role in shoreline processes. For a given H_0 (and T_0), the values of $<\eta>$ on a dissipative beach will be lower than on a reflective or intermediate beach. (This is seen in Fig. 5a where the values of $<\eta>$ for Terschelling and Agate Beach fall below the below the data cluster and the best-fit line.) Earlier work on setup has shown that $<\eta>$ decreases for lower values of γ (Bowen et al., 1968) and that γ values are lower on dissipative sites (Bowen et al., 1968) and, particularly, on lower sloping beaches (Sallenger and Holman, 1985).

The behavior of swash under extremely dissipative conditions is also different than during reflective and intermediate conditions. On low-sloping, high-energy beaches, energy in the incident band is saturated and increases in H_0 contribute only to increases in the infragravity band (Guza and Thornton, 1982; Holman and Sallenger, 1985; Ruessink et al., 1998). This was clearly observed in the swash data when dissipative beaches ($\xi_0<0.3$) were separated from the intermediate and reflective beaches, and S_{inc} and S_{IG} for the two subsets of data were plotted against $(H_0L_0)^{1/2}$ (Fig. 9). On intermediate and reflective beaches, swash in both the incident (Fig. 9c) and infragravity (Fig. 9d) bands increases as H_0 (and T_0) increase. On the dissipative beaches, the magnitude of the infragravity swash grows with increasing H_0 (Fig. 9b) while the incident band swash is completely saturated (Fig. 9a). The saturation of the incident band on dissipative beaches is also revealed by looking at the ratio of S_{inc} to S_{IG}, υ, plotted against ξ_0 (Fig. 10). Cutoff values between dissipative, intermediate, and reflective beaches are defined using an Iribarren equivalent of the Wright and Short (1983) surf-similarity values. Dissipative beaches ($\xi_0<0.3$) are dominated by infragravity energy ($\upsilon<1$) for 90% of the data. The energy on intermediate beaches is closely split between incident- and infragravity-dominated conditions (47% incident energy). On the reflective beaches ($\xi_0>1.25$), the swash is dominated by incident energy ($\upsilon>1$) for 90% of the data. This shows that shoreline motions on reflective beaches are dominated by energy in the incident band while shoreline motions on dissipative beaches are dominated by energy in the infragravity band, again supporting what has been observed and explained using data collected from single sites (Guza and Thornton, 1982; Holman and Sallenger, 1985).

Because total swash on dissipative beaches, S_d, is composed mostly of energy within the infragravity band, it is best parameterized using a form similar to the bulk model describing swash in the infragravity band (Eq. (12)). Modeling both the incident and infragravity bands together,

$$S_d = 0.046(H_0L_0)^{1/2} \quad (17)$$

(Fig. 8b). The correlation for this dissipative-specific parameterization ($\rho^2=0.78$, $\rho^2_{sig}=0.22$) is significantly higher than that for the parameterization of S on dissipative beaches which includes β_f ($\rho^2=0.67$). Additionally, the rms error is reduced from 21.3 to 15.7 cm when β_f is removed from the expression. Using a small subset of data from infragravity-dominated Agate Beach, Ruggiero et al. (2004) found a slope dependence in

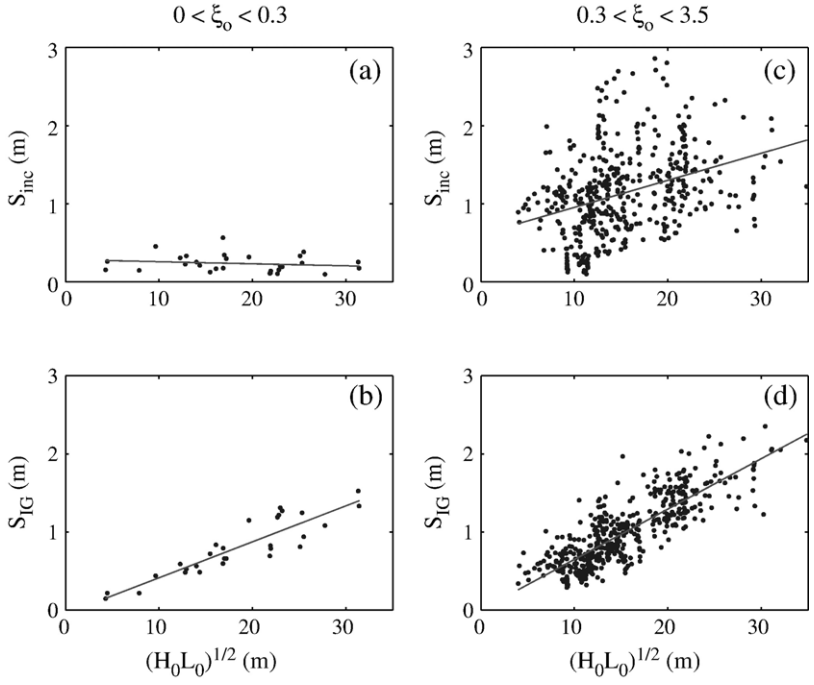

Fig. 9. Incident and infragravity swash plotted against $(H_0L_0)^{1/2}$ for dissipative (a, b) and intermediate/reflective (c, d) beaches. On dissipative beaches, the incident band (a) is saturated while the magnitude of the infragravity band (b) continues to grow with increasing $(H_0L_0)^{1/2}$. On intermediate and reflective beaches, both frequency bands respond to increases in $(H_0L_0)^{1/2}$.

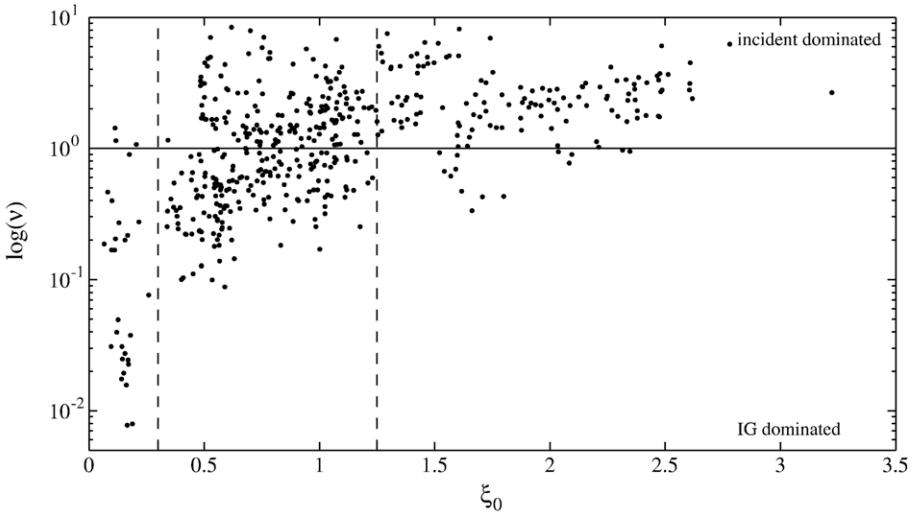

Fig. 10. Ratio of incident to infragravity swash variance (v) plotted against the Iribarren number. The vertical dashed lines mark the cutoff values between dissipative ($\xi_0<0.3$), intermediate, and reflective beaches ($\xi_0>1.25$). Values above the horizontal line at $\log(v)=1$ are incident dominated while those below the line are infragravity dominated.

spatially variable swash. However, when all swash data, including the subset used by Ruggiero et al., are examined together, no significant linear slope dependence exists. It has been suggested by other researchers (Ruessink et al., 1998; Ruggiero et al., 2001) that swash on highly dissipative beaches should be scaled using wave height alone; however, the correlation for this model is only 0.37 and the rms error is larger (29.5 cm). The model using $(H_0L_0)^{1/2}$ has a significantly higher correlation and lower rms error, suggesting that the inclusion of wave period allows for improved predictive capabilities. Based on these dissipative-specific parameterizations and substituting into Eq. (9), runup on sites where $\xi_0<0.3$ may be calculated as

$$R_2 = 0.043(H_0L_0)^{1/2}. \tag{18}$$

The improved performance of this model is given in Table 5. The setup bias for dissipative sites was reduced from −16 to 3 cm. The bias and noise for swash for individual dissipative sites were also significantly reduced. The bias decreased from 29 to 13 cm while the ΔS_{rms} decreased from 34 to 16 cm. The evaluation of the estimators across all sites, using the dissipative-specific parameterizations when $\xi_0<0.3$, is also presented in Table 5.

Table 5
Accuracy of setup, swash and runup parameterizations for dissipative sites (cm)

Experiment	$\overline{\Delta<\eta>}$	$\Delta<\eta>_{rms}$	$\overline{\Delta S}$	ΔS_{rms}	$\overline{\Delta R}$	ΔR_{rms}
Terschelling [a]	8	14	10	12	3	15
Agate Beach	−1	9	16	17	−9	23
Average error, $\xi_0<0.3$	3	12	13	16	−5	21
Average error, all sites	−2	21	33	46	−17	38

	$\overline{<\eta>}$ (cm)	$\overline{S}$ (cm)	$\overline{R}$ (cm)
$\xi_0<0.3$	27	85	84
All sites	49	149	144

Mean observed values of setup, swash, and runup are presented in the last two rows in order to examine mean error magnitudes relative to observed values.

[a] The results of the two Terschelling field campaigns are combined in these statistics.

The final, general expression for runup on all beaches, based on the entire data set and substituting Eqs. (10)–(12) into Eq. (9), is

$$R_2 = 1.1\left(0.35\beta_f(H_0L_0)^{1/2} + \frac{[H_0L_0(0.563\beta_f^2 + 0.004)]^{1/2}}{2}\right) \tag{19}$$

and may be used over the full range of beach conditions. Given the dissipative-specific formulations, it may seem logical for intermediate- and reflective-specific parameterizations as well. However, when conditions where $\xi_0>0.3$ are considered separately, the coefficients of the setup and incident swash parameterization change less than 0.5% and the coefficient of the infragravity parameterization changes ~2.8%. On reflective beaches ($\xi_0>1.25$), where swash is dominated by incident energy, the complete expression for runup 2% exceedence elevations (Eq. (19)), can be simplified by assuming that the infragravity contribution (the 0.004 term) to total runup is negligible. Here, incident swash and setup have the same parametric dependencies and can be combined,

$$R_2 = 0.73\beta_f(H_0L_0)^{1/2}. \tag{20}$$

While this simplified form is more convenient for practical applications, the rms error under reflective conditions is 47 cm, larger than that for the full expression (Eq. (19), rmse=32 cm). Therefore, our final recommendation is the broad use of the full expression (Eq. (19)), with an exception (Eq. (18)) for extremely dissipative conditions.

6. Conclusions

The elevation of extreme runup peaks, given by the 2% exceedence value, R_2, is dependent on the sum of two dynamically different processes, the time-mean setup, $<\eta>$, and swash, defined in terms of the significant swash height, S, and computed as four times the square root of the swash variance. Extreme runup is defined as the sum of setup and half of the total swash excursion (Eqs. (6) and (9)). Empirical formulations for each of the components have been developed using carefully defined water-level, wave, and topography statistics from 10 field experiments spanning a wide range of environmental conditions. This data set represents a major expansion on the range of conditions for which empirical relationships have been tested.

Dimensional setup is best parameterized ($\rho^2=0.48$, rmse= 21.3 cm) using foreshore beach slope, estimated over the region of significant swash activity ($<\eta>\pm S/2$), and offshore wave height and wavelength (Eq. (10)), the dimensionally equivalent form of an Iribarren number dependency. The significant swash excursion can be decomposed into incident ($f_0>0.05$ Hz) and infragravity ($f_0<0.05$ Hz) frequency bands, $S=\sqrt{(S_{\mathrm{inc}})^2+(S_{\mathrm{IG}})^2}$, each of which is be modeled separately. Dimensional incident swash scales with foreshore beach slope, offshore wave height, and offshore wavelength (Eq. (11), $\rho^2=0.44$, rmse=46.9 cm). Dimensional infragravity swash also scaled well with $\beta(H_0L_0)^{1/2}$; however, when foreshore slope was removed from the equation, the correlation of the model improved (Eq. (12), $\rho^2=0.65$, rmse=25.7 cm). Additionally, the use of the surf-zone slope (defined as the average slope from the break point to the mean swash location) in the parameterization offered no significant improvements, even on days when wave breaking was occurring on the sandbar.

The above relationships for setup and swash show large biases under the extreme dissipative conditions of two of the field sites, perhaps reflecting the increasing role of bottom friction on very wide surf zones in the dynamic balances. For Iribarren numbers less than 0.3, setup was best parameterized using only offshore wave conditions (Eq. (16), $\rho^2=0.68$, rmse=11.9 cm). Similarly, the total swash, merging both frequency bands, was best parameterized using only offshore wave height and wavelength (Eq. (17), $\rho^2=0.78$, rmse=15.7 cm).

Substituting the suggested forms of setup and swash, the final parameterization for the 2% exceedence value of runup peaks on all natural beaches is

$$R_2 = 1.1\left(0.35\beta_{\mathrm{f}}(H_0L_0)^{1/2} + \frac{[H_0L_0(0.563\beta_{\mathrm{f}}^2+0.004)]^{1/2}}{2}\right).$$

Under extremely dissipative conditions, estimates of R_2 may be improved using the dissipative-specific parameterization

$$R_2 = 0.043(H_0L_0)^{1/2} \quad \text{for } \xi_0<0.3.$$

The performance of the runup parameterizations was tested at each site using data collected along a single transect. The mean difference between the estimated and measured runup was −17 cm, indicating that the parameterization tends to slightly underestimate the elevation of runup peaks. The rms difference between estimated and measured runup was 38 cm.

The longshore variability of runup was examined during the Delilah, Duck94, and SandyDuck experiments where runup data were collected over extensive longshore arrays. On days when foreshore slope was longshore variable, runup, in particular incident band swash, was also spatially variable. Differences between longshore observed runup and runup predictions made using a single longshore-averaged foreshore slope may be as much as 38% when the foreshore topography is highly three-dimensional (for example, within a megacusp field). Longshore variability in foreshore slope may result in a relative runup error equal to 51% of the fractional variability between the measured and averaged slope.

Acknowledgments

The authors thank Todd Holland, Peter Ruggiero, and Gerben Ruessink for sharing their swash time series and for providing expert knowledge on the details of their experiments. We also thank John Stanley, Cindy Paden, Joe Haxel, Logan Mitchell, David Sedivy, Nick Parazoo, and Dan Clark for their assistance with runup digitization. Wave data for the different experiments were provided by the U.S. Army Corps of Engineers' Field Research Facility, the NOAA National Buoy Data Center, the Coastal Data Information Program, and Britt Raubenheimer. We thank Bob Guza for his thoughtful review of the manuscript. This research was funded by the USGS National Assessment Program.

References

Baldock, T.E., Holmes, P., 1999. Simulation and prediction of swash oscillations on a steep beach. Coastal Engineering 36 (3), 219–242.

Battjes, J.A., 1974. Surf Similarity, Proceedings of the 14th Conference of Coastal Engineering. ASCE, pp. 466–480.

Birkemeier, W.A., Mason, C., 1984. The CRAB: a unique nearshore surveying vehicle. Journal of Surveying Engineering 110, 1–7.

Bowen, A.J., Inman, D.L., Simmons, V.P., 1968. Wave 'set-down' and 'set-up'. Journal of Geophysical Research 73 (8), 2569–2577.

Elgar, S., Herbers, T.H.C., Okihiro, M., Oltman-Shay, J., Guza, R.T., 1992. Observations of infragravity waves. Journal of Geophysical Research 97 (C10), 15573–15577.

Guza, R.T., Thornton, E.B., 1980. Local and shoaled comparisons of sea surface elevations, pressures and velocities. Journal of Geophysical Research 85 (C3), 1524–1530.

Guza, R.T., Thornton, E.B., 1981. Wave set-up on a natural beach. Journal of Geophysical Research 86 (C5), 4133–4137.

Guza, R.T., Thornton, E.B., 1982. Swash oscillations on a natural beach. Journal of Geophysical Research 87 (C1), 483–491.

Hanslow, D., Nielsen, P., 1993. Shoreline set-up on natural beaches. Journal of Coastal Research SI (15), 1–10.

Herbers, T.H.C., Hendrickson, E.J., O'Reily, W.C., 2000. Propagation of swell across a wide continental shelf. Journal of Geophysical Research 105 (C8), 19729–19737.

Holland, K.T., Holman, R.A., 1993. Statistical distribution of swash maxima on natural beaches. Journal of Geophysical Research 98 (C6), 10271–10278.

Holland, K.T., Holman, R.A., 1996. Field observations of beach cusps and swash motions. Marine Geology 134, 77–93.

Holland, K.T., Raubenheimer, B., Guza, R.T., Holman, R.A., 1995. Runup kinematics on a natural beach. Journal of Geophysical Research 100 (C3), 4985–4993.

Holland, K.T., Holman, R.A., Lippmann, T.C., Stanley, J., Plant, N., 1997. Practical use of video imagery in nearshore oceanographic field studies. IEEE Journal of Oceanic Engineering 22 (1), 81–92.

Holman, R.A., 1986. Extreme value statistics for wave run-up on a natural beach. Coastal Engineering 9, 527–544.

Holman, R.A., Bowen, A.J., 1984. Longshore structure of infragravity wave motions. Journal of Geophysical Research 89 (C4), 6446–6452.

Holman, R.A., Guza, R.T., 1984. Measuring run-up on a natural beach. Coastal Engineering 8, 129–140.

Holman, R.A., Sallenger Jr., A.H., 1985. Setup and swash on a natural beach. Journal of Geophysical Research 90 (C1), 945–953.

Howd, P.A., Oltman-Shay, J., Holman, R.A., 1991. Wave variance partitioning in the trough of a barred beach. Journal of Geophysical Research 96 (C7), 12781–12795.

Hunt, I.A., 1959. Design of seawalls and breakwaters. Journal of Waterways and Harbours Division, ASCE 85 (WW3), 123–152.

Iribarren, C.R., Nogales, C., 1949. Protection Des Ports, XVIIth International Naval Congress, Lisbon, pp. 31–80.

Longuet-Higgins, M.S., Stewart, R.W., 1963. A note on wave set-up. Journal of Marine Research 21, 4.

Longuet-Higgins, M.S., Stewart, R.W., 1964. Radiation stresses in water waves; a physical discussion, with applications. Deep-Sea Research 11, 529–562.

Miche, R., 1951. Le pouvoir réfléchissant des ouvrages maritimes exposés à l'action de la houle. Annales des Ponts et Chaussées 121, 285–319.

Nielsen, P., Hanslow, D.J., 1991. Wave runup distributions on natural beaches. Journal of Coastal Research 7 (4), 1139–1152.

Raubenheimer, B., Guza, R.T., 1996. Observations and predictions of run-up. Journal of Geophysical Research 101 (C10), 25575–25587.

Raubenheimer, B., Guza, R.T., Elgar, S., Kobayashi, N., 1995. Swash on a gently sloping beach. Journal of Geophysical Research 100 (C5), 8751–8760.

Raubenheimer, B., Guza, R.T., Elgar, S., 2001. Field observations of wave-driven setdown and setup. Journal of Geophysical Research 106 (C3), 4629–4638.

Ruessink, B.G., Kleinhaus, M.G., van den Beukel, P.G.L., 1998. Observations of swash under highly dissipative conditions. Journal of Geophysical Research 103 (C2), 3111–3118.

Ruggiero, P., Komar, P.D., McDougal, W.G., Marra, J.J., Beach, R.A., 2001. Wave runup, extreme water levels and the erosion of properties backing beaches. Journal of Coastal Research 17 (2), 407–419.

Ruggiero, P., Holman, R.A., Beach, R.A., 2004. Wave run-up on a high-energy dissipative beach. Journal of Geophysical Research 109 (C6).

Sallenger, A.H., 2000. Storm impact scale for barrier islands. Journal of Coastal Research 16 (3), 890–895.

Sallenger Jr., A.H., Holman, R.A., 1985. Wave-energy saturation on a natural beach of variable slope. Journal of Geophysical Research 90 (C6), 11939–11945.

Seymour, R.J., Sessions, M.H., Castel, D., 1985. Automated remote recording and analysis of coastal data. Journal of Waterway, Port, Coastal, and Ocean Engineering 111 (2), 388–400.

Thornton, E.B., Guza, R.T., 1982. Energy saturation and phase speeds measured on a natural beach. Journal of Geophysical Research 87 (C12), 9499–9508.

Thornton, E.B., Guza, R.T., 1983. Transformation of wave height distribution. Journal of Geophysical Research 88 (C10), 5925–5938.

Wright, L.D., Short, A.D., 1983. Morphodynamics of beaches and surf zones in Australia. In: Komar, P.D. (Ed.), CRC Handbook of Coastal Processes and Erosion. CRC Press, Boca Raton, pp. 35–64.